LA-3917-MS

LOS ALAMOS SCIENTIFIC LABORATORY
of the
University of California
LOS ALAMOS • NEW MEXICO

A Multilevel Analysis of the ^{235}U Fission Cross Section

UNITED STATES
ATOMIC ENERGY COMMISSION
CONTRACT W-7405-ENG. 36

Printed in the United States of America. Available from
Clearinghouse for Federal Scientific and Technical Information
National Bureau of Standards, U. S. Department of Commerce
Springfield, Virginia 22151
Price: Printed Copy $3.00; Microfiche $0.65

LA-3917-MS
UC-34, PHYSICS
TID-4500

LOS ALAMOS SCIENTIFIC LABORATORY
of the
University of California
LOS ALAMOS • NEW MEXICO

Report written: April 16, 1968

Report distributed: August 21, 1968

A Multilevel Analysis of the ^{235}U Fission Cross Section

by

James D. Cramer

A MULTILEVEL ANALYSIS OF THE ^{235}U FISSION CROSS SECTION

by

James D. Cramer

ABSTRACT

Resonance parameters for the ^{235}U fission cross section, as measured on the Petrel experiment at the Nevada Test Site, were determined using a multilevel fitting program based on the Wigner-Eisenbud R-Matrix theory.

INTRODUCTION

On the Petrel experiment the fission cross section of ^{235}U was measured.[1] The ^{235}U sample on this experiment was also used to determine the neutron flux above 10 keV. Neutron energies were separated by time of flight in a 200-meter evacuated pipe to the surface. Cross section data from 2 MeV to 20 eV are taken in, typically, 4 msec using this technique.[2] Backgrounds associated with this measurement are extremely low in the resonance region, resulting in deeper valleys between resonances in the fission cross section of ^{235}U than indicated by previous measurements.

It seemed appropriate to fit these data using a multilevel formalism allowing interference between adjacent levels in the same fission channel to describe these deep valleys.

METHOD

The Reich-Moore[3] multilevel fitting technique was used to determine the resonance parameters for these ^{235}U fission data. An approximate trial and error fit of the fission data was achieved using two fission channels and a single value of 40 meV for the capture width. Use of the value of the fission widths from this fit and the capture-to-fission ratio from the ORNL-RPI data of de Saussure et al.[4] to determine a more appropriate value to use for capture width strongly indicated two values, 20 and 45 meV. Assuming that these two widths indicate two entrance channels, we achieved the final multilevel fit by separating the levels with indication of different capture widths into two groups with capture widths of 29 and 45 meV, and assigning to each group two fission channels. Although there is provision in the Reich-Moore code for splitting any one level into two or more channels as is expected statistically for a fraction of the levels, no use of this additional degree of freedom was attempted for this fit.

RESULTS

The upper plot in Fig. 1 shows the results of the fission fit from 18 to 46 eV. The parameters used in the calculated values of the cross section (indicated by the solid line) include the energy of the resonance, the reduced neutron width, the fission width, and the capture width. The points on this figure indicate the experimental values of the fission cross section. The capture cross section was calculated using the Reich-Moore code with the same resonance parameters used in the fission fit.

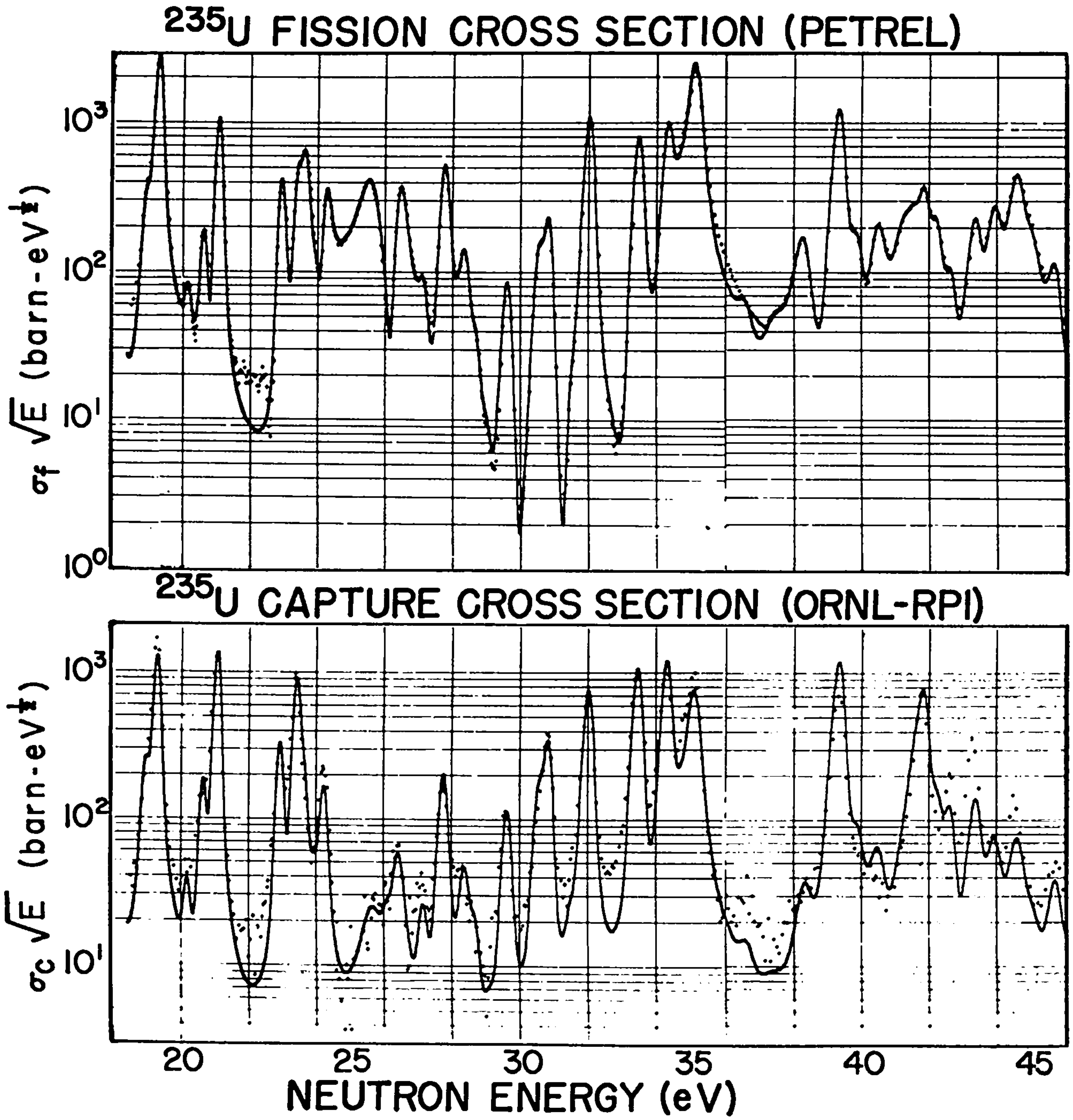

Fig. 1. Upper: Multilevel fit to the Petrel fission data (points) from 18 to 46 eV.

Lower: Multilevel fit to the ORNL-RPI capture data (points) using the same parameters used to fit the fission data above.

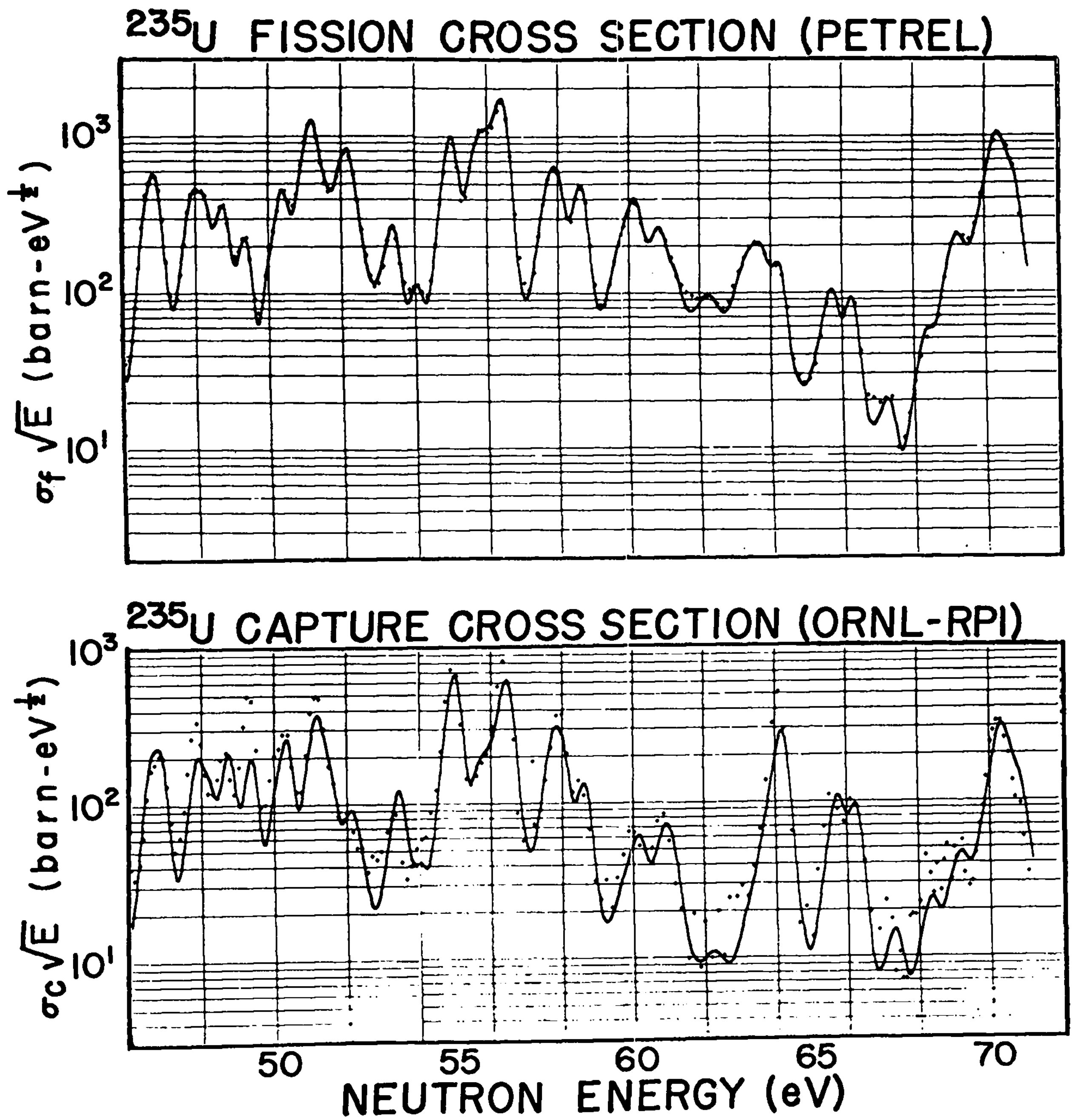

Fig. 2. Upper: Multilevel fit to the Petrel fission data (points) from 46 to 72 eV.

Lower: Multilevel fit to the ORNL-RPI capture data (points) using the same parameters used to fit the fission data above.

The lower plot in this figure shows the results of that calculation (the solid line) compared with the ORNL-RPI capture cross-section data of de Saussure et al.

There are several places in the cross section where the effects of interference can be assumed: the deep valleys in the 30-eV region are fitted with interference between levels. In the region of the 25-eV resonance, interference between only two levels was used to fit the data between 24 and 26 eV. Single level fits have required as many as five levels to fit the cross section in this region. Figure 2 shows the multilevel fit of experimental fission data from 46 to 72 eV. Again the calculated capture cross-section is compared with the ORNL-RPI experimental data.

A total of 80 levels was used in this analysis, 49 with assigned capture widths of 45 meV in two channels and 31 with assigned capture widths of 29 meV in two channels.

Figure 3 is a plot of the number of levels used in the fitting as a function of energy. The slope of the best straight line through this plot indicates an average level spacing of 0.663 eV. Above 65 eV the slope of the plot breaks off, indicating the loss of resolution of individual levels at that point.

A plot of the partial sum of reduced neutron widths, Γ_n^o, determined by the multilevel analysis is shown in Fig. 4. The strength function can be determined from the slope of the best straight line through this plot and, as indicated, is 2×10^{-4}. This value is consistent with what would be expected for two entrance channels in the statistical model.

The distribution of fission widths for all levels is shown in Fig. 5. The solid lines indicate the integral of the Porter-Thomas distribution from x to ∞ for 1, 3, and 6 degrees of freedom. As shown the average fission width is 130.9 meV.

The integral form of the Porter-Thomas distribution of reduced neutron widths is shown in Fig. 6. The solid line indicates the P-T distribution with 1 degree of freedom. There may be slight indication of two populations in this distribution. However, in work with mock cross-section data, deviations from the Porter-Thomas distribution similar to those indicated here are observed when the weaker levels

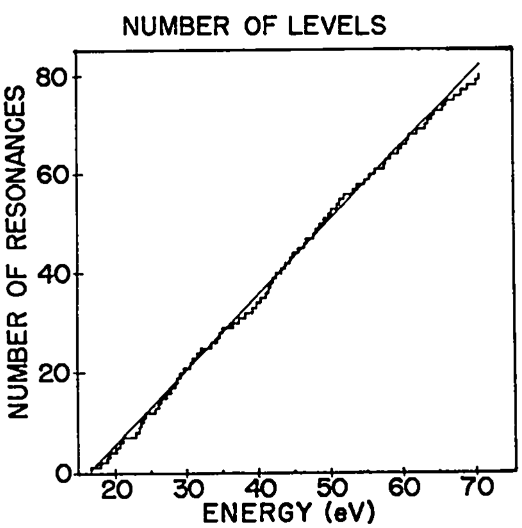

Fig. 3. The number of levels observed in the analysis.

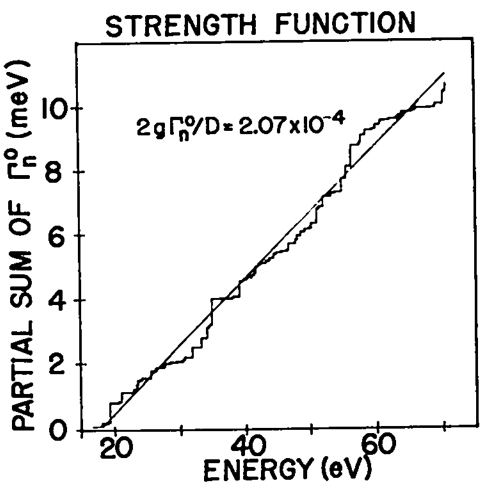

Fig. 4. The partial sum of the reduced neutron widths.

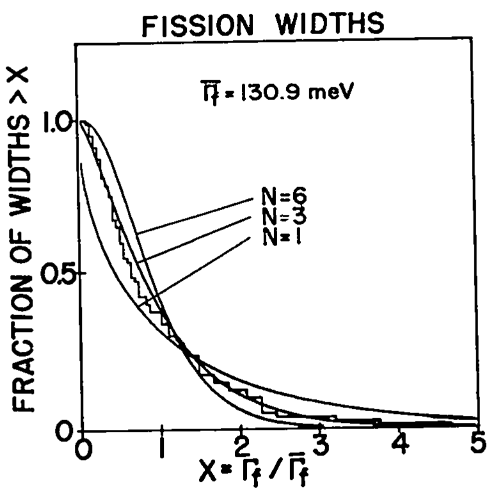

Fig. 5. The fraction of fission widths greater than X.

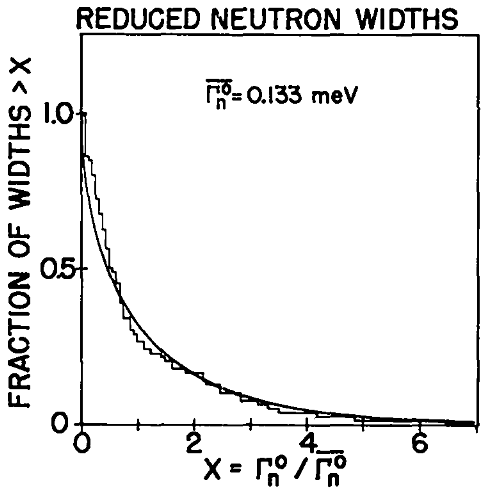

Fig. 6. The fraction of reduced neutron widths greater than X.

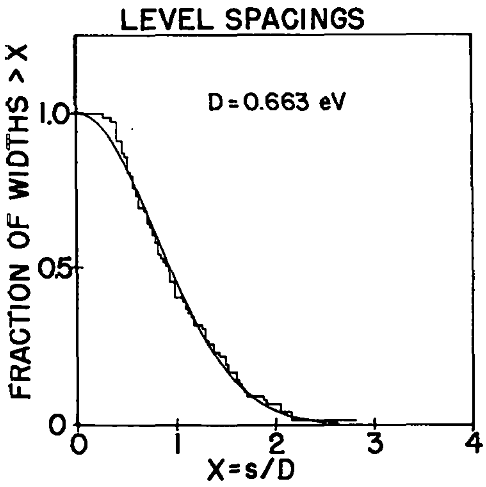

Fig. 7. Fraction of level spacings, S, greater than S/D.

are eliminated from the analysis. The distribution of level spacing, S, greater than S/D is shown in Fig. 7. A plot of the Wigner distribution is shown as a solid line. There is strong indication of missing closely spaced levels on this plot.

The parameters used in this analysis are listed in Table I. Parity is assigned to each fission width, determining the type of interference required between levels in the same channel.

CONCLUSION

Although there seems to be much evidence for two entrance channels in this analysis, there is no indication that spins could be assigned to each level correctly with more than 50% certainty. It appears that a future analysis of these data requiring a simultaneous fit to a good neutron capture measurement such as the ORNL-RPI measurement could lead to spin assignments for each level.

ACKNOWLEDGMENTS

The author gratefully acknowledges the advice of J. A. Farrell and D. W. Bergen in completing this analysis.

REFERENCES

1. W. K. Brown, D. W. Bergen, and J. D. Cramer, Report CONF-660303, Book 2, p. 971 (1966).
2. A. Hemmendinger, Phys. Today 18, 8, p. 17 (1965).
3. C. W. Reich and M. S. Moore, Phys. Rev. 3, 929 (1958).
4. G. de Saussure et al., ORNL-TM-1804 (1967).

TABLE I - Resonance Parameters of ^{235}U

Energy (eV)	Γ_n^o (meV)	Γ_f (meV) Chan 1	Chan 2	Chan 3	Chan 4	Γ_γ (meV)
16.67	0.06	-85				29
18.05	0.098	+140				29
18.97	0.065			+60		45
19.295	0.56		-65			29
20.19	0.0085	+50				29
20.67	0.04		+30			29
21.085	0.290	+23				29
22.95	0.095	-38				29
23.44	0.15	+14				29
23.62	0.122		-90			29
23.97	0.015			-100		45
24.245	0.05		-55			29
25.62	0.22		+610			29
26.15	0.0015		-60			29
26.51	0.105		+225			29

TABLE I (continued)

Energy (eV)	Γ_n^o (meV)	Γ_f (meV) Chan 1	Chan 2	Chan 3	Chan 4	Γ_γ (meV)
27.18	0.011	+75				29
27.8	0.115	+75				29
28.42	0.028	-100				29
28.73	0.0062	+70				29
29.15	0.0007				+120	45
29.68	0.03				-35	45
30.61	0.045				-42	45
30.88	0.08		+20			29
31.55	0.003		-40			29
32.07	0.3		+42			29
33.52	0.29		+22			29
34.36	0.33			-42		45
34.74	0.09			+175		45
35.15	0.82				-180	45
36.6	0.008			-225		45
37.4	0.0065			-425		45
38.36	0.058				+275	45
39.37	0.47			+50		45
39.92	0.053			-150		45
40.51	0.065			+200		45
41.3	0.072			-275		45
41.61	0.06			+90		45
41.88	0.2			-25		45
42.27	0.07			+95		45
42.65	0.036				+35	45
43.43	0.072			-75		45
43.98	0.085				-170	45
44.64	0.125	+175				29
45.04	0.055		-300			29
45.78	0.027		+100			29
46.65	0.046	+35				29
46.92	0.193				+120	45
47.94	0.105				-90	45
48.25	0.132			-150		45
48.82	0.12				+73	45
49.44	0.087			+50		45
50.05	0.028				-90	45
50.4	0.150			-75		45
51.26	0.45			+160		45
51.6	0.067	+60				29
52.22	0.33		-300			29
53.5	0.094			-100		45
54.05	0.036				-200	45
55.05	0.42			-65		45
55.8	0.38				+300	45
56.52	0.65				-135	45
57.78	0.095			+70		45
58.02	0.22				+110	45
58.68	0.169		+115			29
59.75	0.033			+300		45
60.22	0.134		-200			29
60.95	0.1				-200	45
61.22	0.04				-150	45
62.35	0.039			-500		45
63.46	0.045				+325	45

TABLE I (continued)

Energy (eV)	Γ_n^o (meV)	Γ_f (meV) Chan 1	Chan 2	Chan 3	Chan 4	Γ_γ (meV)
63.8	0.07		+250			29
64.28	0.094				+30	45
64.70	0.003			-60		45
65.8	0.049			+45		45
66.32	0.052			+45		45
67.4	0.0077				-60	45
68.4	0.017		-70			29
69.27	0.1			-250		45
70.42	0.38				-140	45
70.88	0.25			+200		45